One Pulse Spin-locking in NQR *

B. Bandyopadhyay, G. B. Furman, S. D. Goren, C. Korn, and A. I. Shames

Department of Physics, Ben-Gurion University of the Negev, P.O. Box 653, 84105 Be'er Sheva, Israel

Z. Naturforsch. **51a**, 357–362 (1996); received December 12, 1995

The response of a quadrupolar spin system in zero applied magnetic field to a long π_f pulse, for both single crystal and polycrystalline samples possessing broad Lorentzian-shaped resonance lines has been studied. The dependencies of magnetization on frequency offset, linewidth and power are investigated both theoretically and experimentally. The problem of the effective field direction in both single crystal and polycrystalline samples is also discussed. For a polycrystalline cuprous oxide (Cu_2O) sample it is observed that the magnetization after a long pulse in on-resonance condition does not become zero for time $t \gg T_2$, in agreement with theoretical results. It has also been shown that the magnetization increases with increase in the width of the resonance line as well as with the decrease in the excitation power.

Key words: NQR, one pulse spin-locking, Cu_2O.

1. Introduction

The spin-locking technique in NMR and NQR experiments is usually implemented by applying a phase-shifted two pulse sequence [1]. The same effect can be achieved in both NMR [2] and NQR [3, 4] with a long off-resonance pulse. In this case, the magnetization does not decay during the time $T_2 \ll t \ll T_1$ (T_1 and T_2 are spin-lattice and spin-spin relaxation times, respectively). According to [3] and [4], no signal should be observed after an excitation lasting a few times T_2 when applied at on-resonance condition. The theoretical results are in good agreement with the experimental data for samples having narrow NQR lines [3, 4].

In the present paper, we study the resonance of a quadrupolar spin system with arbitrary spin in zero applied magnetic field to a long π_f pulse in both single crystal and polycrystalline samples.

2. Theory

Let us consider a spin system with spin $S \geq 1$ and retain in the Hamiltonian $\mathcal{H}(t)$ only those terms which are necessary to the description of the dynamics of the spin system during the time interval $t < T_1$. The evolution of the spin system influenced by a π_f field can be described by the state operator $\varrho(t)$ which is a solution of the equation ($\hbar = 1$)

$$i \frac{\mathrm{d}\varrho(t)}{\mathrm{d}t} = [\mathcal{H}(t), \varrho(t)] \tag{1}$$

with the Hamiltonian

$$\mathcal{H}(t) = \mathcal{H}_\mathrm{Q} + \mathcal{H}_\mathrm{dd} + \mathcal{H}_{\pi_f}(t) . \tag{2}$$

Here

$$\mathcal{H}_\mathrm{Q} = \sum_i \frac{eQq_{zz}}{4S(2S-1)} \left[3S_{iz}^2 - \boldsymbol{S}_i^2 + \frac{\eta}{2}(S_{i+}^2 + S_{i-}^2) \right] \tag{3}$$

represents the interaction of the nuclear quadrupole moment with the electric field gradient (EFG) in the principal EFG frame, eQq_{zz} and η are the quadrupole coupling constant and the asymmetry parameter of the EFG, respectively. $\mathcal{H}_\mathrm{dd}$ is the Hamiltonian of the dipole-dipole interaction. $\mathcal{H}_{\pi_f}(t)$ defines the interaction between the spin system and the π_f field as

$$\mathcal{H}_{\pi_f}(t) = \omega_1 (\boldsymbol{m} \cdot \boldsymbol{S}) \cos \omega_{\pi_f} t , \tag{4}$$

where $\omega_1 = \gamma \mathrm{H}_1$, γ is the gyromagnetic ratio, H_1 is the amplitude of π_f field, and the unit vector $\boldsymbol{m}$ determines the direction of the π_f field, given in the principal EFG frame as

$$\boldsymbol{m} = \{\sin\theta \cos\varphi, \sin\theta \sin\varphi, \cos\theta\} . \tag{5}$$

To take into account the time dependent part of the Hamiltonian (2), it is advantageous to consider (1) in the interaction representation [5] with an effective

* Presented at the XIIIth International Symposium on Nuclear Quadrupole Interactions, Providence, Rhode Island, USA, July 23–28, 1995.

Reprint requests to Dr. A. I. Shames.

0932-0784 / 96 / 0500-0357 $ 06.00 © – Verlag der Zeitschrift für Naturforschung, D-72072 Tübingen

time independent Hamiltonian

$$\mathcal{H}_e = \Delta I_3 + \omega_1 \cdot f(\theta, \varphi, \eta) I_1 + \mathcal{H}_d, \tag{6}$$

where $\Delta = \omega_{rf} - \omega_Q$ is off-set, ω_Q is the resonant NQR frequency (Fig. 1),

$$f(\theta, \varphi, \eta) = (R R^* + K K^*)^{1/2}, \tag{7}$$

and $R = R(\theta, \varphi, \eta)$ and $K = K(\theta, \varphi, \eta)$ are matrix elements of the operator $(\boldsymbol{m} \cdot \boldsymbol{S})$ in $\mathcal{H}_Q$ representation. $\mathcal{H}_d$ is the secular part of the dipole-dipole interaction Hamiltonian relative to $\mathcal{H}_Q$ [5]. The components of the Hermitian operator $\mathbf{I}(I_1, I_2, I_3)$, defined in [5], satisfy the commutation relations

$$[I_i, I_j] = \varepsilon_{i,j,k} \cdot i I_k . \tag{8}$$

The effective Hamiltonian (6) can be represented in the form

$$\mathcal{H}_e = \omega_e (\boldsymbol{e} \cdot \mathbf{I}) + \mathcal{H}_d, \tag{9}$$

where ω_e is the effective frequency

$$\omega_e = [\Delta^2 + \omega_1^2 f(\theta, \varphi, \eta)]^{1/2}. \tag{10}$$

$\boldsymbol{e}$ is the unit vector along the effective field $\boldsymbol{H}_e = \dfrac{\omega_e}{\gamma} \boldsymbol{e}$ and can be expressed as

$$\boldsymbol{e} = \frac{1}{\omega_e} \left\{ \left[\Delta^2 - \omega_1 f\left(\frac{\pi}{2}, 0, 0\right)(\boldsymbol{m} \cdot \boldsymbol{k}) \right] \cdot \boldsymbol{k} + \omega_1 f\left(\frac{\pi}{2}, 0, 0\right) \boldsymbol{m} \right\}, \tag{11}$$

where $\boldsymbol{k}$ is the unit vector along the offset field. We stress that the vector $\boldsymbol{k}$ in general does not coincide with the z axis of the principal EFG frame, i.e.,

$$(\boldsymbol{m} \cdot \boldsymbol{k}) = \left[1 - f^2(\theta, \varphi, \eta) / f^2\left(\frac{\pi}{2}, 0, 0\right) \right]^{1/2}. \tag{12}$$

In general, the unit vectors $\boldsymbol{e}$, $\boldsymbol{m}$ and the z-axis of the principal EFG frame do not lie in the same plane From (11) we can obtain the angle between the rf field and the effective field along which the magnetization is locked:

$$\cos\alpha = (\boldsymbol{m} \cdot \boldsymbol{e}) = \frac{1}{\omega_e} \{ \Delta (\boldsymbol{m} \cdot \boldsymbol{k}) + \omega_1 [1 - (\boldsymbol{m} \cdot \boldsymbol{k})^2] \}. \tag{13}$$

The effective Hamiltonian being time independent, it may be assumed that during the time $\sim T_2$ after the beginning of the rf pulse the spin system will reach a quasi-equilibrium state [1] with the state operator given as (in the high temperature approximation)

$$\varrho_e = 1 - \beta_e \mathcal{H}_e \tag{14}$$

for $\omega_e \sim \omega_{loc}$, where $\omega_{loc} = \mathrm{Tr}\{\mathcal{H}_d^2\}/\mathrm{Tr}\{S^2\}$ is the dipolar linewidth,

and $$\varrho_e = 1 - \beta_s \omega_e (\boldsymbol{e} \cdot \mathbf{I}) - \beta_d \mathcal{H}_d \tag{15}$$

for $\omega_e \gg \omega_{loc}$. Here β_e, β_s and β_d are inverse temperatures of the spin, Zeeman and dipole systems respectively, in the interaction representation.

Case I. $\omega_e \sim \omega_{loc}$

In this case, during a time $\sim T_2$ we can neglect the absorption of the rf field energy by the spin system and use the low enery conservation

$$\mathrm{Tr}\{\varrho(0) \mathcal{H}_e\} = \mathrm{Tr}\{\varrho_e \mathcal{H}_e\}, \tag{16}$$

which gives

$$\frac{\beta_e}{\beta_L} = \frac{\omega_Q \omega_e (\boldsymbol{k} \cdot \boldsymbol{e})}{\omega_e^2 + \omega_{loc}^2}, \tag{17}$$

where $\varrho(0)$ is initial state operator given by

$$\varrho(0) = 1 - \beta_L \mathcal{H}_Q, \tag{18}$$

in which $\beta_L = \dfrac{1}{k T_L}$ and T_L is the lattice temperature.

Using (11), (14) and (17), we obtain the observed component of the quasi-equilibrium magnetization

$$\frac{M_m}{M_0} = \frac{\omega_e (\boldsymbol{k} \cdot \boldsymbol{e})(\boldsymbol{m} \cdot \boldsymbol{e})}{\omega_e^2 + \omega_{loc}^2}, \tag{19}$$

where M_0 is the magnetization immediately after the 90° pulse.

Equation (19) shows the decrease of the observed quasi-equilibrium magnetization, indicating that the energy exchange between the quadrupole and dipole-dipole reservoirs takes place during the time $\sim T_2$. Moreover, the magnetization is now aligned in the direction of the effective field with simultaneous disappearance of the magnetization components which were previously perpendicular to the effective field. In the on-resonance case we see from (11) and (19) that the observed magnetization is zero. A similar observation has already been made earlier for a sample possessing a narrow NQR line [3, 4]. In a more general case, i.e., taking into account the distribution of resonant NQR frequencies (Δ_r) over the real line with non-zero linewidth (δ), (19) must averaged over the line:

$$\left\langle \frac{M_m}{M_0} \right\rangle_{\Delta_r} = \int_{-\infty}^{+\infty} \frac{M_m}{M_0} g(\Delta_r) \, \mathrm{d}\Delta_r \tag{20}$$

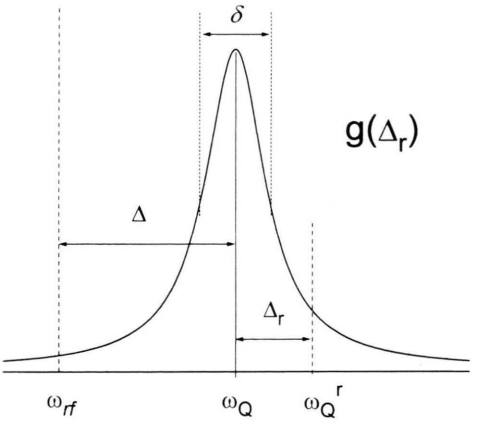

Fig. 1. The Lorentzian distribution $g(\Delta_r)$ given by (21) as a function of linewidth (δ) and frequency deviation (Δ_r). Δ, the frequency off-set, is the difference between the resonance frequency (ω_Q) and the rf frequency (ω_{rf}).

where $g(\Delta_r)$ is a normalized function of Δ_r (Figure 1). The numerical analysis of such an averaging for the Gaussian lines has already been done by Pratt et al. [4]. However, they have not discussed the on-resonance case. Here, let us consider the Lorentzian distribution of frequencies over a line having width δ,

$$g(\Delta_r) = \frac{1}{\pi}\frac{\delta}{\delta^2 + \Delta_r^2}. \tag{21}$$

After averaging according to (20), we obtain

$$\left\langle \frac{M_m}{M_0} \right\rangle_{\Delta_r} = (\boldsymbol{m}\cdot\boldsymbol{k})[1 - b(b+1)A] + \frac{\omega_1^*}{\delta}[1-(\boldsymbol{m}\cdot\boldsymbol{k})^2]A, \tag{22}$$

where

$$A = \frac{1}{d}[a^2 + (b-1)^2], \tag{23}$$

$$a = \frac{\Delta}{\delta}, \tag{24}$$

$$b^2 = \frac{1}{\delta^2}\{\omega_1^{*2}[1-(\boldsymbol{m}\cdot\boldsymbol{k})^2] + \omega_{loc}^2\}, \tag{25}$$

$$d = (a^2 + b^2 - 1)^2 + 4a^2, \tag{26}$$

and $$\omega_1^* = \omega_1 \cdot f\left(\frac{\pi}{2}, 0, 0\right). \tag{27}$$

In the case of on-resonance $\Delta = 0$, and it follows from (22–27) that the magnetization

$$\left\langle \frac{M_m}{M_0} \right\rangle_{\Delta_r} = \frac{(\boldsymbol{m}\cdot\boldsymbol{k})}{1+b} \tag{28}$$

is not zero.

For polycrystalline samples, the quasi-equilibrium magnetization given by (22) must be averaged over the angles θ and φ as

$$\langle \ldots \rangle_{\theta,\varphi} \equiv \frac{1}{2\pi}\int d\theta \int d\varphi\, |\sin\theta| \ldots. \tag{29}$$

For example, let us consider a spin system with $S = 3/2$. In this case

$$f(\theta,\varphi,\eta) = \frac{1}{\sqrt{1+\eta^2/3}} \cdot \left[\frac{\eta^2}{3} + \frac{1}{4}\sin^2\theta(3-\eta^2+2\eta\cos 2\varphi)\right]^{1/2}. \tag{30}$$

From (28), for $\eta = 0$ and after averaging as in (29), we obtain

$$\left\langle \left\langle \frac{M_m}{M_0} \right\rangle_{\Delta_r} \right\rangle_{\theta,\varphi} = \frac{4\delta}{3\omega_1}\left[\sqrt{\tfrac{3}{4}\omega_1^2 + \omega_{loc}^2} - \omega_{loc} - \delta \ln\left(\frac{\delta + \sqrt{\frac{3}{4}\omega_1^2 + \omega_{loc}^2}}{\delta + \omega_{loc}}\right)\right]. \tag{31}$$

In the case of polycrystalline sample having a narrow resonance line we may obtain the angle between the rf coil and the effective field direction,

$$\langle (\boldsymbol{m}\cdot\boldsymbol{e})\rangle_{\theta,\varphi} = \frac{3\Delta^2}{4\omega_1^2} + \left(\frac{1}{2} - \frac{3\Delta^2}{4\omega_1^2}\right)\arcsin\left(\frac{1}{\sqrt{1+\frac{3\Delta^2}{4\omega_1^2}}}\right). \tag{32}$$

Case II. $\omega_e \gg \omega_{loc}$

In this case, the spin system is characterized by two motion integrals, namely $\omega_e(\boldsymbol{e}\cdot\boldsymbol{I})$ and $\mathcal{H}_d$. Using the conservation law we obtain

$$\frac{\beta_s}{\beta_L} = \frac{\omega_Q}{\omega_e}(\boldsymbol{k}\cdot\boldsymbol{e}) \tag{33}$$

and $$\beta_d \approx 0. \tag{34}$$

From (11), (15), and (33) we obtain the observed magnetization

$$\frac{M_m}{M_0} = (\boldsymbol{k}\cdot\boldsymbol{e})(\boldsymbol{m}\cdot\boldsymbol{e}). \tag{35}$$

This result shows that, in contrast to the previous case (given by (19)), the decrease of the magnetization is now entirely determined by its alignment along the direction of the effective field at time $\sim T_2$. Equa-

tions (22) to (27) are valid with the substitution of b by $b_1 = \omega_1^{*2}[1 - (\boldsymbol{k} \cdot \boldsymbol{m})^2]/\delta^2$.

3. Experimental

All measurements wer performed at room temperature on a sample of polycrystalline cuprous oxide (Cu_2O) in zero applied magnetic field using a Tecmag Libra pulsed NMR spectrometer. The sample was subjected to $\pi/$ pulses of variable length, frequency and power. To avoid the drift of the resonant frequency due to increase of temperature during a long signal acquisition time with high power pulses, the sample was placed in a continuous dry air flow. In order to reduce the errors in the magnetization measurement, the FID signals were treated by Fourier transformation, baseline and phase corrections and then the magnetization values were obtained from the peak intensities of the absorption lines. Two resonance lines were found at frequencies of about 24.06 MHz (^{65}Cu) and 26.01 MHz (^{63}Cu). Both these lines exhibited the Lorentzian line shape with linewidth HHFW = 10 ± 1 kHz and relaxation times $T_1 = 166 \pm 35$ ms and $T_2 = 60 \pm 10$ μs for ^{65}Cu; $T_1 = 116 \pm 7$ ms and $T_2 = 40 \pm 5$ μs for ^{63}Cu. The results as described below were the same for both copper isotopes, but all detailed measurements were made on the more intensive ^{63}Cu NQR line.

The experiments were mostly done at a fixed $\pi/$ pulse amplitude such that the 90° pulse length was 4 μs (or $3.9 \cdot 10^5$ rad/s). The pulses at this amplitude and with a duration of 300 μs were used for long pulse experiments. The pulse repetition rate was set at five times T_1. The dependence of the magnetization on the off-resonance excitation by the long pulse was observed upwards from 30 kHz below the exact value of the resonant NQR frequency in steps of 5 kHz until 30 kHz above resonance (Figure 2). The points in Fig. 2 are drawn at the real off-set values measured as a function of the shift of the absorption line from the resonant frequency found for the short 90° pulse. The result of two independent measurements are plotted on the same graph. This figure clearly shows that the magnetization measured after a long pulse is not equal to zero even at the exact on-resonance condition. Moreover, the position of the minimum in the intensities is found to be shifted from the zero off-set position in the direction of higher frequency (negative off-set according to Figure 1).

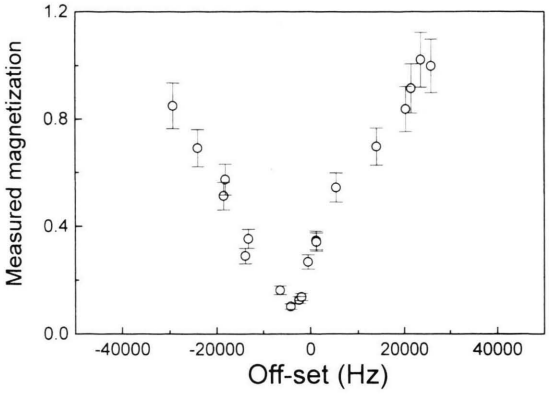

Fig. 2. Intensity of the magnetization observed after a long 300 μs pulse as a function of the frequency off-set. The intensities have been normalized to that of the 90° pulse.

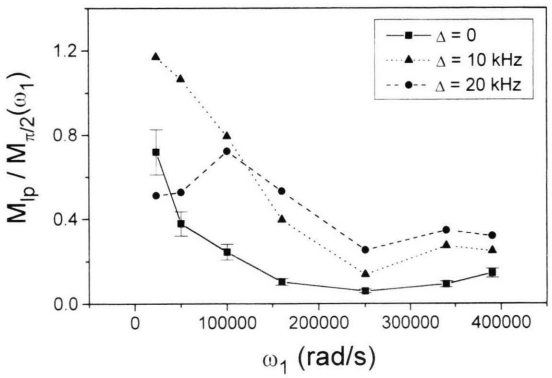

Fig. 3. Magnetization observed after a long pulse of varying power (ω_1), normalized to the magnetization due to excitation by a corresponding 90° pulse, plotted as a function of power and frequency off-set (Δ).

Figure 3 is a plot of intensities after excitation by 300 μs $\pi/$ pulses of varying power at different values of off-set. For each power setting (ω_1), the intensities were normalized with respect to the corresponding 90° pulse. This graph shows the unusual increase of magnetization for both the on- and off-resonance cases when the power is reduced. The drop in the magnetization at the low power side of the scale for large off-sets is also very remarkable.

4. Discussion

Both the theoretical and experimental results presented above show that for the dipolar coupled spin

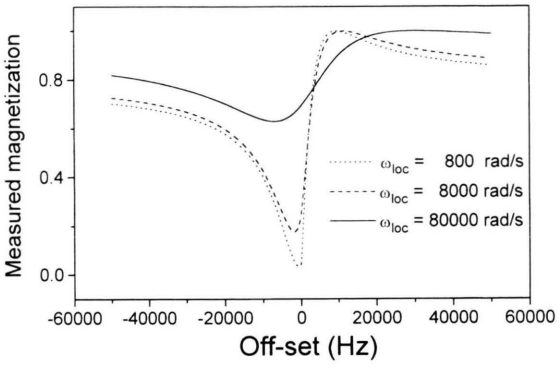

Fig. 4. Dependence of the magnetization on off-set values. Simulation of (22) averaged over different orientations for the polycrystalline sample having $S = 3/2$, $\eta = 0$ for three different values of ω_{loc}.

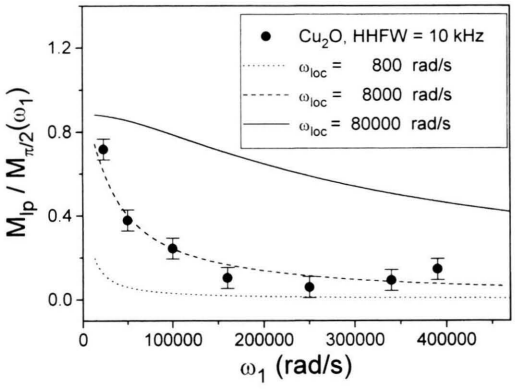

Fig. 5. Dependence of the on-resonance magnetization on the ν_1 power. Simulation of (31) for three different values of ω_{loc}. The circles denote experimental data.

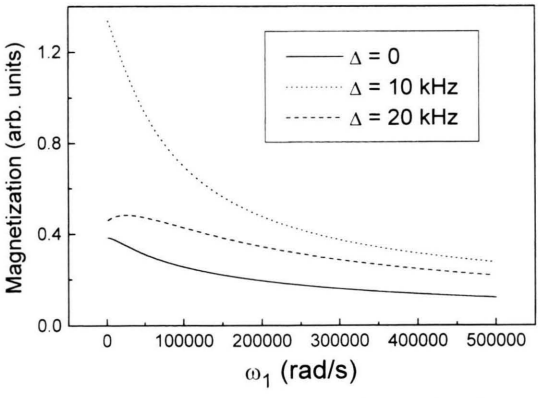

Fig. 6. Dependence of the magnetization on the ν_1 power for three different values of off-set Δ. Simulation of (22) averaged over different orientations for the same polycrystalline sample.

system excited by a long pulse, there exists a non-zero magnetization. The excitation of such a system by a single long pulse creates a spin-locking state for both the on- and off-resonance cases; the magnetization is locked along the direction of the effective field. The orientation of the effective field with respect to the ν_1 coil axis depends on the excitation parameters such as frequency off-set and amplitude of the long pulse. Equations (11) and (13) clearly show that the variation of these parameters changes the orientation of the quasiequilibrium magnetization.

Figure 4 shows the computer simulation of (22), averaged over different orientations for the polycrystalline sample having $S = 3/2$, $\eta = 0$. It is found that the magnetization at on-resonance increases with increase of the width of the resonance line. The shift of the minimum from the position of zero off-set becomes more pronounced for the broad lines. Both these effects have been observed experimentally (Figure 2).

Let us now analyze the power dependence of the magnetization for the on-resonance case. The lines in Fig. 5 show the magnetization values calculated according to (31) for different dipolar broadening. For the sake of simplicity we show only the case $\delta = \omega_{loc}$. For the narrow NQR line, the magnetization after a long pulse at high power is close to zero and grows slightly with power reduction. For samples possessing broad lines, we get a higher on-resonance magnetization and its growth due to power reduction becomes more pronounced. The simulation with the parameter $\delta = \omega_{loc} = 8000$ rad/s (Fig. 5, dashed line) gives a good fit to the experimental data for cuprous oxide (Fig. 5, circles). The analysis of the power dependence data at different off-set values for polycrystalline samples (Fig. 3) requires simulation of (22) averaged over all orientations. The results of such an averaging with the parameters above are plotted in Figure 6. Although we were unable to normalize the data to fit them to the experimental results, these curves qualitatively describe both the upward shift of the power dependence for the off-resonance case and the drop of the magnetization at low powers for the large off-set that has been observed experimentally (Figure 3).

6. Conclusions

For systems possessing a Lorentzian-shaped NQR line, the spin-locking state with non-zero magnetiza-

tion can be obtained by applying a single long ν_1 pulse for both on- and off-resonance excitation. The magnetization is oriented along the direction of the effective field which depends on the excitation parameters such as frequency off-set and applied power. It has also been shown that the magnetization increases with increase in the width of the resonance line as well as with decrease in ν_1 power of the excitation.

Acknowledgements

The authors are grateful to the Wolfson Foundation for providing the financial support which enabled the purchase of the Tecmag spectrometer. We also thank Prof. S. Vega for helpful discussion and Dr. E. M. Kunoff for discussions and friendly support in manuscript preparation. This research was partially supported by a grant from the Israeli Ministry of Immigrant Absorption.

[1] M. Goldman, Spin Temperature and Nuclear Magnetic Resonance in Solids, Clarendon Press, Oxford 1970.
[2] C. P. Slichter and W. C. Holton, Phys. Rev. **122,** 1701 (1961).
[3] J. C. Pratt, P. Raghunatan, and C. A. McDowell, J. Chem. Phys. **61,** 1016 (1974).
[4] J. C. Pratt, P. Raghunatan, and C. A. McDowell, J. Magn. Res. **20,** 313 (1975).
[5] N. E. Ainbinder and G. B. Furman, Sov. Phys. JETP **58,** 575 (1983).